Title

A Time-Walk Correction Method for PET Detectors Based on Leading Edge Discriminators

Journal

IEEE Transactions on Radiation and Plasma Medical Sciences, 1(5)

ISSN

2469-7311

Authors

Du, Junwei
Schmall, Jeffrey P
Judenhofer, Martin S
et al.

Publication Date

2017-09-01

DOI

10.1109/trpms.2017.2726534

Peer reviewed

HHS Public Access

Author manuscript

IEEE Trans Radiat Plasma Med Sci. Author manuscript; available in PMC 2018 September 01.

Published in final edited form as:

IEEE Trans Radiat Plasma Med Sci. 2017 September ; 1(5): 385–390. doi:10.1109/TRPMS.2017.2726534.

A Time-Walk Correction Method for PET Detectors Based on Leading Edge Discriminators

Junwei Du [Senior Member, IEEE],
Department of Biomedical Engineering, University of California, Davis, CA 95616 USA

Jeffrey P. Schmall,
Department of Biomedical Engineering, University of California

Martin S. Judenhofer [Senior Member, IEEE],
Department of Biomedical Engineering, University of California, Davis, CA 95616 USA

Kun Di,
Department of Biomedical Engineering, University of California, Davis, CA 95616 USA

Yongfeng Yang, and
Department of Biomedical Engineering, University of California, Davis, CA 95616 USA

Simon R. Cherry [Fellow, IEEE]
Department of Biomedical Engineering, University of California, Davis, CA 95616 USA

Abstract

The leading edge timing pick-off technique is the simplest timing extraction method for PET detectors. Due to the inherent time-walk of the leading edge technique, corrections should be made to improve timing resolution, especially for time-of-flight PET. Time-walk correction can be done by utilizing the relationship between the threshold crossing time and the event energy on an event by event basis. In this paper, a time-walk correction method is proposed and evaluated using timing information from two identical detectors both using leading edge discriminators. This differs from other techniques that use an external dedicated reference detector, such as a fast PMT-based detector using constant fraction techniques to pick-off timing information. In our proposed method, one detector was used as reference detector to correct the time-walk of the other detector. Time-walk in the reference detector was minimized by using events within a small energy window (508.5 – 513.5 keV). To validate this method, a coincidence detector pair was assembled using two SensL MicroFB SiPMs and two 2.5 mm × 2.5 mm × 20 mm polished LYSO crystals. Coincidence timing resolutions using different time pick-off techniques were obtained at a bias voltage of 27.5 V and a fixed temperature of 20 °C. The coincidence timing resolution without time-walk correction were 389.0 ± 12.0 ps (425 –650 keV energy window) and 670.2 ± 16.2 ps (250–750 keV energy window). The timing resolution with time-walk correction improved to 367.3 ± 0.5 ps (425 – 650 keV) and 413.7 ± 0.9 ps (250 – 750 keV). For comparison, timing resolutions were 442.8 ± 12.8 ps (425 – 650 keV) and 476.0 ± 13.0 ps (250 – 750 keV) using constant fraction

Jeffrey P. Schmall now is with the University of Pennsylvania, Philadelphia, PA 19104 USA.

techniques, and 367.3 ± 0.4 ps (425 – 650 keV) and 413.4 ± 0.9 ps (250 – 750 keV) using a reference detector based on the constant fraction technique. These results show that the proposed leading edge based time-walk correction method works well. Timing resolution obtained using this method was equivalent to that obtained using a reference detector and was better than that obtained using constant fraction discriminators.

Index Terms

Leading edge discriminator; Time-walk correction; Timing resolution; PET; Time of Flight

I. Introduction

Different algorithms and techniques have been proposed to estimate the gamma photon arrival times in PET to achieve an optimized coincidence timing resolution (CTR) [1]–[10]. Among these methods, digital methods and statistical methods have advantages over the two traditional analog methods, the leading edge discriminator (LED) and the constant fraction discriminator (CFD) [11], but are also more complicated, computational intense, and difficult to be implemented in hardware, such as within application-specific integrated circuits (ASIC) or field-programmable gate arrays (FPGA). CFD has been considered as a gold standard for obtaining timing information in PET application for many years, but it needs more components to implement, especially the delay line, which is difficult to incorporate in compact integrated circuit (IC) chips. Non-delay line CFDs also have been proposed, however, this requires more components to replace the delay line [12]. The variable delay that is necessary for different pulse shapes to obtain the best timing resolution makes its use even more difficult [13]–[14]. Although digital CFDs can be implemented inside an FPGA and can use variable delay lengths, this implementation needs a very fast analog-to-digital converter (ADC), which is power hungry and expensive [6], [15]. An LED with a low-level threshold applied to the leading edge of the signal is the simplest time pick-off method. The time for crossing the threshold suffers time-walk, but can be corrected by using the relationship between the threshold crossing time, and the energy, on an event-by-event basis [11], [16]. Recent work has shown that the timing resolution obtained using a LED is better than that obtained using a CFD, when a lower threshold (several photons) is used and a narrow energy window (with a width of tens of keV) was applied to select events [17].

For clinical PET scanners, the energy window is typically 425 keV – 650 keV, and it can be as wide as ~250 – 750 keV for small-animal PET scanners. For such wide energy windows, time-walk correction is required to improve timing resolution. This is critical for applications requiring good timing resolution to lower the random coincidence event rate and obtain time-of-flight information, and imaging applications that use wide energy windows with a large range of pulse amplitudes to improve sensitivity, such as high-resolution, small-animal PET. The relationship between the event energy and the time to cross a pre-set threshold can be obtained by using a precision reference detector; data from the coincidence detector pair can be used to correct the detector of interest. In a real scanner, a calibration probe can be used as a reference detector [18]. In this case, the electronics

either needs to be modified during the time-walk correction process, or requires provision for spare connections for the external probe. Also, the calibration process must be performed with some frequency due to changes in the characteristics of the detector, such as aging effects and change of temperature or bias voltage for SiPM- or APD-based detectors. For detectors with readout electronics already incorporated, such as SensL's Matrix9 and Hamamatsu's MPPC modules [19]–[20], reading out the timing and energy signals in coincidence with a calibration reference detector cannot be done without modifying the electronics. Hence, the time-walk correction needs to be done using the timing information generated by the detector itself.

In this work, we proposed and evaluated a time-walk correction method based on two detectors both using LEDs to generate timing information. This method is self-calibrated, as no extra reference detectors are needed to generate the relationship between threshold crossing time and event energy. The timing resolution obtained using our proposed method was also compared with results obtained using CFD and CFD-based correction methods at four different energy thresholds (15 keV, 100 keV, 200 keV and 300 keV).

II. Materials and Methods

A. SiPM and LYSO-based detector

Two detectors were assembled using two MicroFB SiPM evaluation boards (MicroFB-SMTPA-30035, SensL Ltd., Cork, Ireland) and two 2.5 mm × 2.5 mm × 20 mm LYSO crystals (Crystal Photonics, Inc., FL). Each evaluation board contains one MicroFB SiPM pixel (as shown in Fig.1 (top)), which has an active area of 3.0 × 3.0 mm^2 with 4774 microcells, each 35 × 35 μm^2 in size with a fill factor of 64%. The MicroFB SiPMs are UV/blue enhanced light sensors with peak sensitivity at 420 nm [21], well matching the emission spectrum of LYSO [22]. Their photon detection efficiency (PDE) is 31% at a bias voltage of 27.0 V and a temperature of 21 °C.

The two LYSO crystals were wrapped using several layers of Teflon to maximize the light output and coupled to the SiPM using optical grease (Saint Gobain BC-630). With a view to real application in a PET scanner, 20 mm long crystals were used in these experiments, although it is well known that better timing resolution can be obtained using shorter crystals [23].

B. Coincidence timing measurement

Each MicroFB SiPM evaluation board was mounted on a custom front-end board as shown in Fig. 1 (top), and a schematic of the experiment setup is shown in Fig. 1 (bottom). The two LYSO crystals were placed head on to mimic the situation in real scanner. To easily align the two crystals and the radiation source, a 3D printed holder was fabricated to hold the detectors, crystals and the radiation source.

The MicroFB SiPM has both a fast and a standard output. In our experiments, the standard output was used to simplify the readout, as the signal from the fast output is 2 – 4% of that from the standard output and the fast output requires extra transformers and amplifiers with

ultra-high bandwidth [21]. This can be a drawback in terms of the electronics complexity, cost and power consumption at the scanner level.

The signal from the standard output was amplified by an AD8045-based (1 GHz bandwidth, Analog Devices, Inc.) transimpedance amplifier with a feedback resistor of 130 Ohms. The amplified signal was split and one arm was fed into a CAEN spectroscopy amplifier (N568B) for energy information, and the other arm was fed into an LED/CFD (ORTEC 584) for timing information. The ORTEC 584 can work in either LED mode or CFD mode. The outputs of the ORTEC 584s were sent to a time-to-amplitude converter (TAC, ORTEC 566). The output of the N568B and TAC were digitized by a power DAQ board, with 14-bit ADCs [24].

C. Time walk correction method

It is impossible to correct the time-walk of one detector using another detector as a reference detector, when both detectors utilize LEDs to generate time information and events occur over a wide energy range. Our approach was to use events from one detector within a very narrow energy range (which we referred to as “bin size”) around the 511 keV photopeak and treat this detector as a reference detector to correct the time-walk of another detector.

Fig. 2 (top) (black line) shows the energy spectra of detector 1. The low energy cut of the energy spectra is ~ 15 keV, which is limited by the LED module used. If detector 1 is used as a reference detector, the 2D histogram of energy and threshold crossing time of events obtained from detector 2 is shown in Fig. 2 (middle). It is obvious, for events with a given energy, the threshold crossing times varies over a wide range, hence, the relationship between the two cannot be found. Fig. 2 (bottom) shows the relationship between energy and threshold crossing time of detector 2 when detector 1 was used as a reference detector and a 5 keV energy window (511 ± 2.5 keV) was used to select events from detector 1. An obvious relationship between energy and threshold crossing time can now be observed.

Instead of a directly fitting the data shown in Fig.2 (bottom), which is difficult as the data is distributed in two dimensions, the events were rebinned according to their energy and an energy bin size. Gaussian fits were applied to the timing spectra of the events belonging to each energy bin; the center of the energy bin and the peak position of the timing spectra were calculated. A piecewise cubic hermite interpolating polynomial fit (pchip, Matlab 2012) was applied to the center of the energy bin and the peak position of the timing spectra data to find the relationship between event energy and threshold crossing time, as shown in Fig. 2 (bottom) blue line. The fitted function was then applied to the acquired data to correct the time-walk on an event by event basis. The use of a linear fit was also studied, but the performance was not as good, hence, the results using the linear fit are not presented.

For the CFD-based time-walk correction, one detector used the CFD technique and the other used the LED technique to generate timing information. The CFD based detector was used as a reference detector and a 5 keV energy window around the 511 keV photopeak was also applied to select events from the reference detector. A relationship between the energy and threshold crossing time similar to the one shown in Fig. 2 (c) was obtained (not shown). To reduce the statistical error, 50M events were collected for each study.

III. Results

A. Effect of energy threshold on the relationship between event energy and threshold crossing time

Fig. 3 shows the relationship between event energy and threshold crossing time for detector 1. The four lines, obtained at different thresholds, cross at an energy of 511 keV which was set to 0. The threshold crossing time of events with lower (higher) energy was earlier (later) than that of events with an energy of 511 keV, due to the nature of LED technique [11]. The relationships between event energy and threshold crossing time obtained for detector 2 was similar to those of detector 1 and are not shown.

It is expected that the higher the threshold, the steeper the slope of the relationship, because the time-walk of the LED is increased at higher thresholds. The relationship between energy and threshold, obtained at a threshold of 15 keV was fairly flat over a small energy range around 511 keV. It is likely to be even flatter using a lower energy threshold. To get better timing resolution without time-walk correction, a lower threshold should be used and a narrow energy window should be applied to select data, as has been previously presented in many publications [13], [17], [25]–[27].

B. Effect of energy windows on timing resolution

Figure 4 shows the timing resolution versus the energy window width obtained using CFD and LED methods for time pick-off with a threshold of 15 keV. The center of the energy windows was at 511 keV. The timing resolution increases with increasing width of the energy window, both for the CFD and LED. The timing resolution obtained using the LED (without time-walk correction) degrades faster than that obtained using CFD technique, especially above 300 keV energy window width due to the contribution of the strong time-walk effects (see Fig 2). The timing resolution obtained using the LED technique was better than that obtained using CFD when the energy window width was narrower than 350 keV, corresponding to an energy window of 336 – 686 keV, which is consistent with other published data [17].

C. Effect of energy bin size

Figure 5 shows the obtained coincidence timing resolution using different energy bin sizes. The energy bin size (energy window) was used to select events with energy around the 511 keV photopeak for the reference detector and then rebin the events for the detector being corrected for finding the relationship between the event energy and threshold crossing time.

The coincidence timing resolution increases slightly with increasing bin size, due to 1) time-walk of the events from the reference detector, 2) decrease in precision of the pchip fit to the relationship between event energy and threshold crossing time. The timing resolution obtained using a bin size of 0.5 keV and 1 keV is also poorer due to the poor counting statistics and increased statistical error, which leads to difficulties in fitting the data. However, the timing resolution only varied between 365 ps and 370 ps, confirming that the result is quite insensitive to the bin size and large energy bins can be used.

D. Timing resolution

Timing spectra obtained at an energy threshold of 15 keV and for two different energy windows using the LED technique are shown in Fig. 6 (top). The red and blue lines are the results without time-walk correction, while the black and green lines are the results with time-walk correction respectively. Clearly, the results with time-walk correction are better and the time-walk correction provides a more significant improvement when the energy window was wider. The timing spectrum without time-walk correction and using 250 – 750 keV energy window to select data (blue line) has a broad tail, which was caused by Compton events. The broad tail made the timing spectra non-Gaussian in shape and disappeared after time-walk correction was applied to the data.

Figure 6 (bottom) shows the timing resolution obtained using different time pick-off methods and different time-walk correction methods. The legends are explained in Table I. The threshold of the LED was 15 keV and two different energy windows (425 – 650 keV and 250 – 750 keV) were applied to select events. When a narrow energy window was used, the timing resolution obtained using the LED was better than that obtained using the CFD, even without time-walk correction. The timing resolution obtained using LED technique and with time-walk correction was better than that obtained using the CFD using both energy windows, and the timing resolution obtained using the two different time-walk correction methods, LED based self-correction method and reference detector based correction method, were similar.

Table II lists the timing resolution versus threshold of the LED. The timing resolution obtained using the LED technique increases with increasing threshold [17], [26], while that obtained using the CFD was nearly constant at different thresholds. Timing resolutions obtained using LED_Cor and CFD_Cor are the same. This demonstrates that our proposed LED based time-walk correction method works as well as using a dedicated reference detector based on the CFD technique to generate timing information.

IV. Conclusion and Discussion

A self-correction time-walk method was proposed and evaluated for PET detectors using the LED technique to generate the timing information. The timing resolution obtained using our proposed method was the same as that obtained using a dedicated reference detector based on CFD technique, but our method has the advantage that it does not need an external reference detector, electronics modification nor a dedicated calibration process.

The coincidence timing resolution obtained was 389.0 ± 12.0 ps (425 – 650 keV) and 670.2 ± 16.2 ps (250 – 750 keV) without time-walk correction using a 15 keV threshold. The timing resolution was improved to 367.3 ± 0.5 ps (425 – 650 keV) and 413.7 ± 0.9 ps (250 – 750 keV) with time-walk correction. Timing resolutions were 442.8 ± 12.8 ps (425 – 650 keV) and 476.0 ± 13.0 ps (250 – 750 keV) using a CFD, and 367.3 ± 0.4 ps (425 – 650 keV) and 413.4 ± 0.9 ps (250 – 750 keV) using a reference detector based on a CFD.

The timing resolution degraded with increasing energy threshold for the LED, consistent with other results [17], [26]. The best timing resolution was obtained at a threshold of 15

keV among the four tested thresholds (15 keV, 100 keV, 200 keV, and 300 keV). We believe even better timing resolution can be obtained using lower threshold, but this was not tested in this paper. A threshold of 15 keV can be implemented in most state-of-the-art PET scanners, such as SiPM-based PET scanners. The timing resolutions obtained using the LED with time-walk correction were better than those obtained using a CFD by using a 15 keV threshold, which is consistent with other results [17].

The best timing resolution we obtained was 367.3 ± 0.5 ps (425 – 650 keV energy window and 15 keV energy threshold for LED). Better results have been obtained with similar SiPMs and crystals, however we did not optimize the bias voltage for timing performance and our measurement were carried out at a temperature of 20 ° C. For SiPMs, the timing resolution varies with bias voltage and better timing resolution can be obtained at lower temperature, as the noise of SiPMs is decreased [28]–[29].

We also have used our proposed method to correct the timing resolution of two PET detector modules based on large-area SiPM arrays and crystal arrays [19], [30]. Our proposed method worked well and the timing resolution was improved to 4.2 ± 0.1 ns from 11.2 ± 0.2 ns [19].

With the dramatic improvements in data transfer speed that have occurred in recent years (such as USB 3.1 which has a transfer rate up to 1.25 GB/s), and improvements in date storage speeds using solid state drives (SSD), it is feasible to collect single events from the PET scanner [31]–[32]. As the event time-stamps are included in the event data, our proposed LED-based time-walk correction method can be applied to these data to improve the timing resolution without any additional measurements from the PET scanner.

Acknowledgments

The authors wish to thanks Steve Buckley, Wade Appelman and Carl Jackson from SensL Ltd. (Cork, Ireland) for useful discussions and providing the SiPMs.

This work was supported in part by NIH Grant R01 EB019439.

References

1. Abbiati R, Geraci A, Ripamonti G. A weighted least mean squares linear algorithm for energy and occurrence time measurement of pulse. IEEE Trans. Nucl. Sci. Jun.2007 54:629–34.
2. Kim H, Kao CM, Xie Q, Chen CT, Zhou L, Tang F, Frisch H, Moses WW, Choong WS. A multi-threshold sampling method for TOF-PET signal processing. Nucl. Instrum. Methods Phys. Res. A. Apr.2009 602:618–621. [PubMed: 19690623]
3. Joly, B., Montarou, G., Lecoq, J., Bohner, G., Crouau, M., Brossard, M., Vert, PE. Test and optimization of timing algorithms for PET detectors with digital sampling front-end; Proc. IEEE Nuclear Science Symp. Medical Imaging Conf. Rec; 2008. p. 4078-4085.
4. Hua W, Choi Y, Hong K, Kang J, Jung J, Huh Y, Lim H, Kim S, Min B, Kim B. A simple and improved digital timing method for positron emission tomography. Nucl. Instr. Meth. Phys. Res. A. Jun.2010 622:219–224.
5. Monzo JM, Esteve R, Lerche CW, Ferrando N, Toledo J, Aliaga RJ, Herrero V, Mora FJ. Digital signal processing techniques to improve time resolution in positron emission tomography. IEEE Trans. on Nucl. Sci. Aug; 2011 58(4):1613–1620.

6. Cho S, Grazioso R, Zhang N, Aykac M, Schmand M. Digital timing: sampling frequency, anti-aliasing filter and signal interpolation filter dependence on timing resolution. Phys. Med. Biol. Nov. 2011 56:7569–7583. [PubMed: 22086164]
7. Seifert S, van Dam HT, Vinke R, Dendooven P, Löhner H, Beekman FJ, Schaart DR. A comprehensive model to predict the timing resolution of SiPM-based scintillation detectors: theory and experimental validation. IEEE Trans. on Nucl. Sci. Feb; 2012 59(1):190–204.
8. Yeom J, Vinke R, Spanoudaki V, Hong K, Levin CS. Readout electronics and data acquisition of a positron emission tomography time-of-flight detector module with waveform digitizer. IEEE Trans. on Nucl. Sci. Oct; 2013 60(51):3735–3741.
9. Derenzo S, Choong W, Moses WW. Fundamental limits of scintillation detector timing precision. Phys. Med. Biol. May.2014 59:3261–3286. [PubMed: 24874216]
10. Seifert S, Schaart DR. Improving the time resolution of TOF-PET detectors by double-sided readout. IEEE Trans. on Nucl. Sci. Feb; 2015 62(1):3–11.
11. Paulus TJ. Timing electronics and fast timing methods with scintillation detectors. IEEE Trans. on Nucl. Sci. Jun; 1985 32(34):1242–1249.
12. Kim S, Ko G, Kwon S, Lee J. Development of a non-delay line constant fraction discriminator based on the Padé approximant for time-of-flight positron emission tomography scanners. J. Inst. Jan.2015 10:P01005.
13. Ito M, Lee J, Lee J. Timing performance study of new fast PMTs with LYSO for time-of-flight PET. IEEE Trans. on Nucl. Sci. Feb; 2013 60(1):30–37.
14. KO G, Lee J. Performance characterization of high quantum efficiency metal package photomultiplier tubes for time-of-flight and high-resolution PET applications. Med. Phys. Jan; 2015 42(1):510–520. [PubMed: 25563289]
15. Jager M, Butz T. FPGA implementation of digital constant fraction algorithm with fractional delay for optimal time resolution. Nucl. Instr. Meth. Phys. Res. A. Jan.2012 674:24–27.
16. Deng Z, Lan A, Sun X, Bircher C, Liu Y, Shao Y. Development of an eight-channel time-based readout ASIC for PET applications. IEEE Trans. Nucl. Sci. Dec; 2011 58(6):3212–3218.
17. Xu, T., Wen, J., Wang, Q., Wei, Q., Ma, T., Liu, Y., Tai, Y. A novel submillimeter resolution PET detector with TOF capability; Proc. IEEE Nuclear Science Symp. Medical Imaging Conf. Rec; 2013. p. 1-5.
18. Moses WW, Thompson CJ. Timing calibration in PET using a time alignment probe. IEEE Trans. Nucl. Sci. Oct; 2006 53(5):2660–2665.
19. Du J, Schmall J, Yang Y, Di K, Roncali E, Mitchell GS, Buckley S, Jackson C, Cherry SR. Evaluation of Matrix9 silicon photomultiplier array for small-animal PET. Med. Phys. Feb; 2015 42(2):585–599. [PubMed: 25652479]
20. Adachi, S., Nakamura, S., Hirayanagi, M., Suzuki, H., Uchiyama, T., Baba, T., Watanabe, M., Omura, T. Development of MPPC array module; Proc. IEEE Nuclear Science Symp. Medical Imaging Conf. Rec; 2014. p. 1-3.
21. Jackson C, O'Neill K, Wall L, McGarvey B. High volume SiPM production, performance and reliability. Opt. Eng. Aug.2014 53(8):081909.
22. Du J, Wang Y, Zhang L, Zhou Z, Xu Z, Wang X. Physical properties of LYSO scintillator for NN-PET detectors. BMEI. Oct.2009 1:314–318.
23. Gundacker S, Knapitsch A, Auffray E, Jarron P, Meyer T, Lecoq P. Time resolution deterioration with increasing crystal length in a TOF-PET system. Nucl. Instr. Meth. Phys. Res. A. Nov.2013 737:92–100.
24. Judenhofer M, Pichler B, Cherry SR. Evaluation of high performance data acquisition boards for simultaneous sampling of fast signals from PET detectors. Phys. Med. Biol. Jan; 2005 50(1):29–44. [PubMed: 15715420]
25. Kim C, McDaniel DL, Ganin A. Time-of-flight PET detector based on multi-pixel photon counter and its challenges. IEEE Trans. on Nucl. Sci. Feb; 2011 58(1):3–8.
26. O'Neill K, Pavlov N, Dolinsky S, Jackson C. SensL new fast timing silicon photomultiplier. Proceedings of Science - International Workshop on New Photon-detectors. Jun.2012 :1–7.
27. Grant A, Levin CS. A new dual threshold time-over-threshold circuit for fast timing in PET. Phys. Med. Biol. Jun.2014 59:3421–3430. [PubMed: 24889105]

28. Yeom J, Vinke R, Levin CS. Optimizing timing performance of silicon photomultiplier-based scintillation detectors. Phys. Med. Biol. Jan.2013 58:1207–1220. [PubMed: 23369872]

29. Gola A, Piemonte C, Tarolli A. Analog circuit for timing measurements with large area SiPMs coupled to LYSO crystals. IEEE Trans. on Nucl. Sci. Apr; 2013 60(2):1296–1302.

30. Du J, Schmall J, Di K, Yang Y, Judenhofer M, Bec J, Buckley S, Jackson C, Cherry SR. Design and optimization of a high-resolution PET detector module for small-animal PET based on a 12 × 12 silicon photomultiplier array, Biomedical Physics & Engineering Express. Nov.2015 1(4): 045003.

31. Tetrault M, Oliver JF, Bergeron M, Lecomte R, Fontaine R. Real time coincidence detection engine for high count rate timestamp based PET. IEEE Trans. on Nucl. Sci. Feb; 2010 57(1):117–124.

32. Isobe, T., Yamada, R., Shimizu, K., Saito, A., Ote, K., Sakai, K., Moriya, T., Yamauchi, H., Omura, T., Watanabe, M. Development of a new brain PET scanner based on single event data acquisition; Proc. IEEE Nuclear Science Symp. Medical Imaging Conf. Rec; 2012. p. 3540-3543.

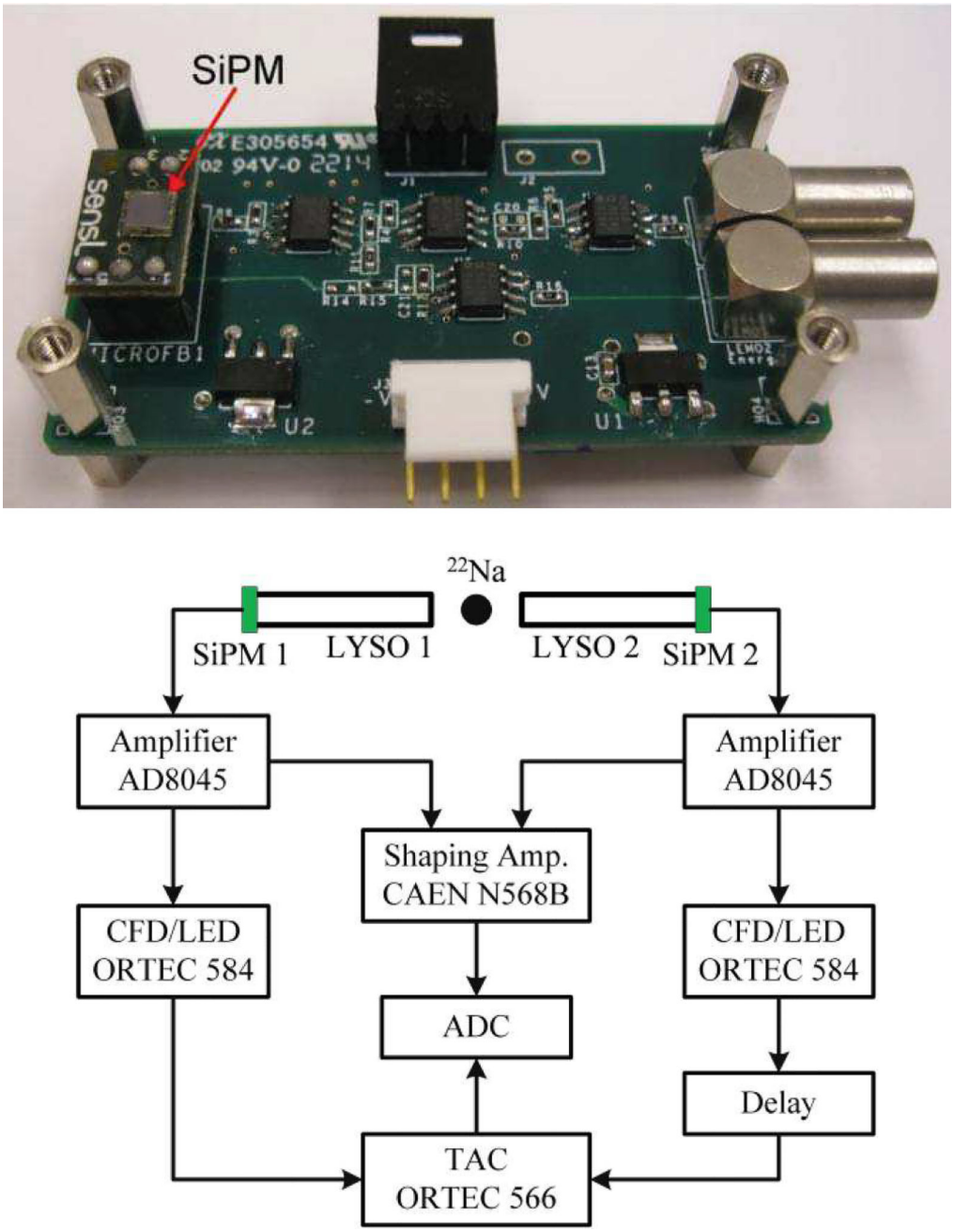

Fig. 1.
(top) Picture of the SiPM and frond-end board, and (bottom) schematic of the coincidence timing measurement setup.

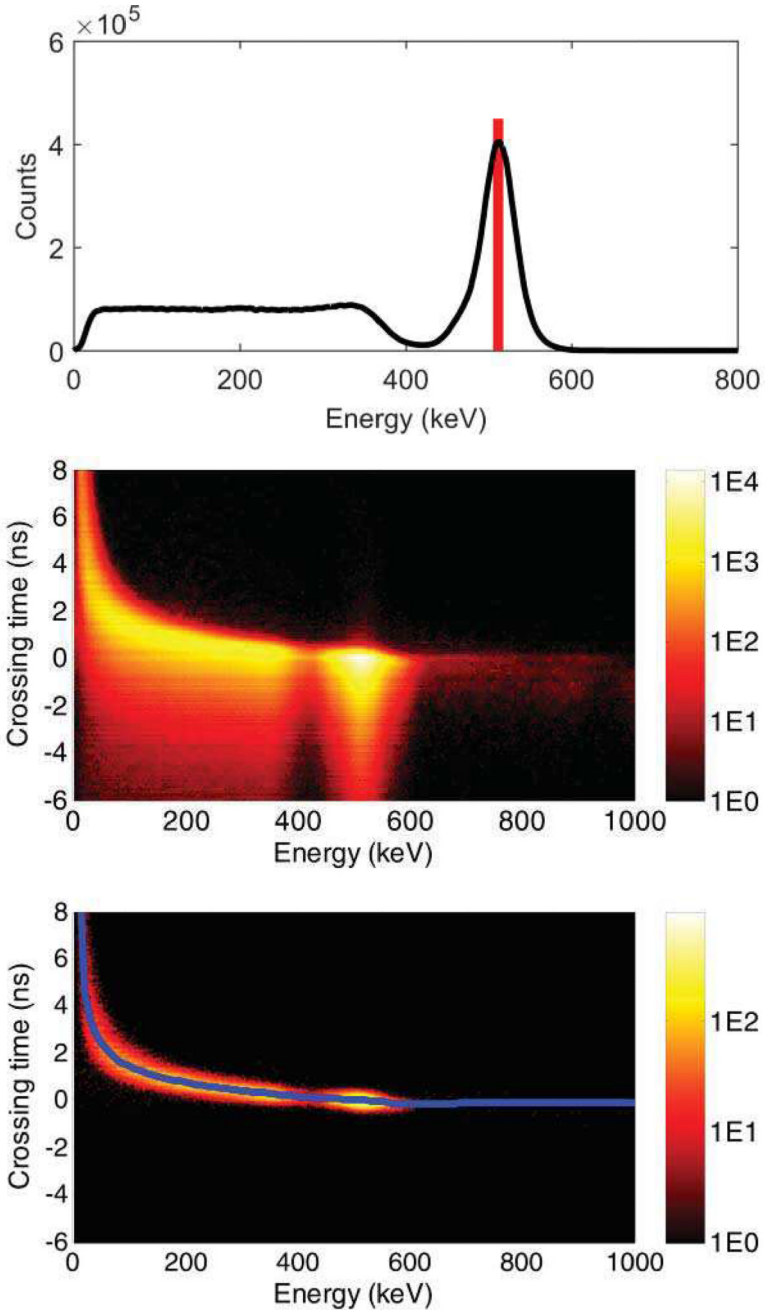

Fig. 2.

(top) Energy spectra of SiPM 1. The relationship between energy and threshold crossing timing of SiPM 2 (middle) before and (bottom) after a narrow energy window was applied to events from SiPM 1. The blue line shows the fit between energy and threshold crossing time, which is then used to correct the time-walk.

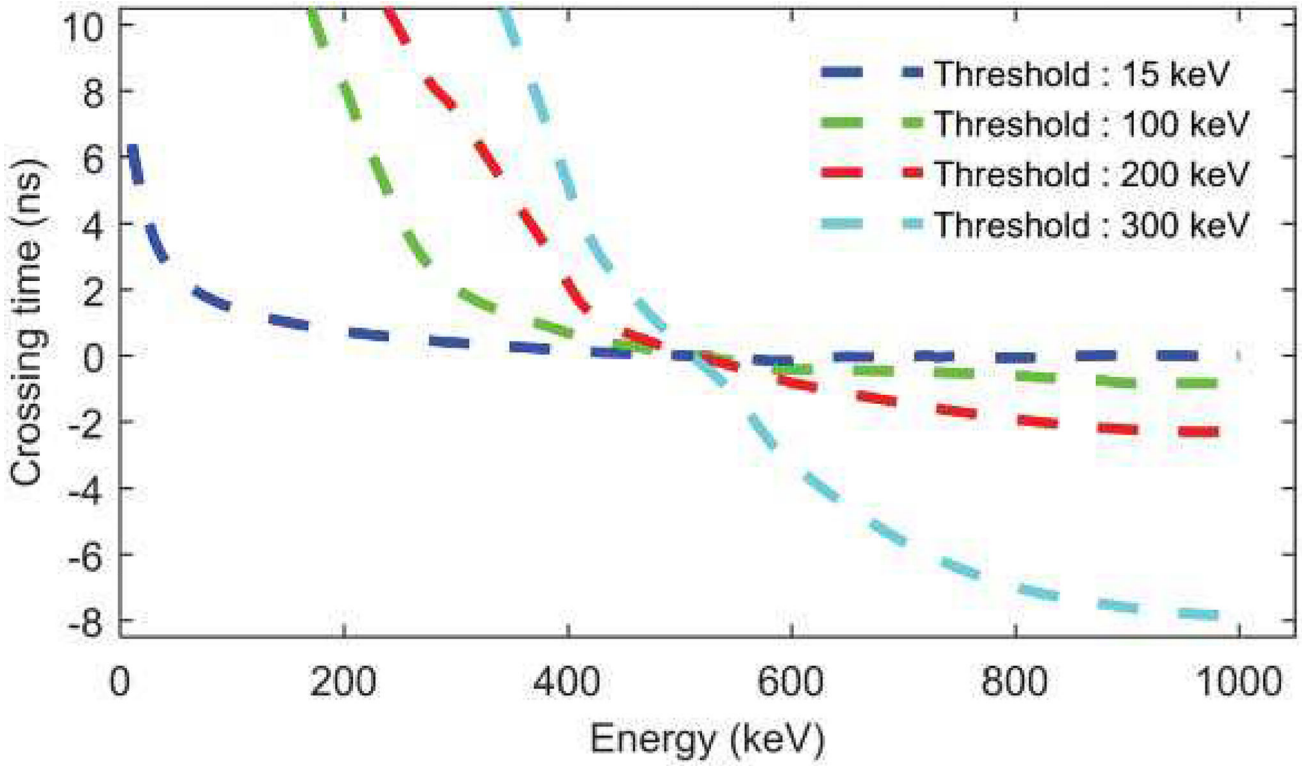

Fig. 3.
Relationship between event energy and threshold crossing time of detector 1.

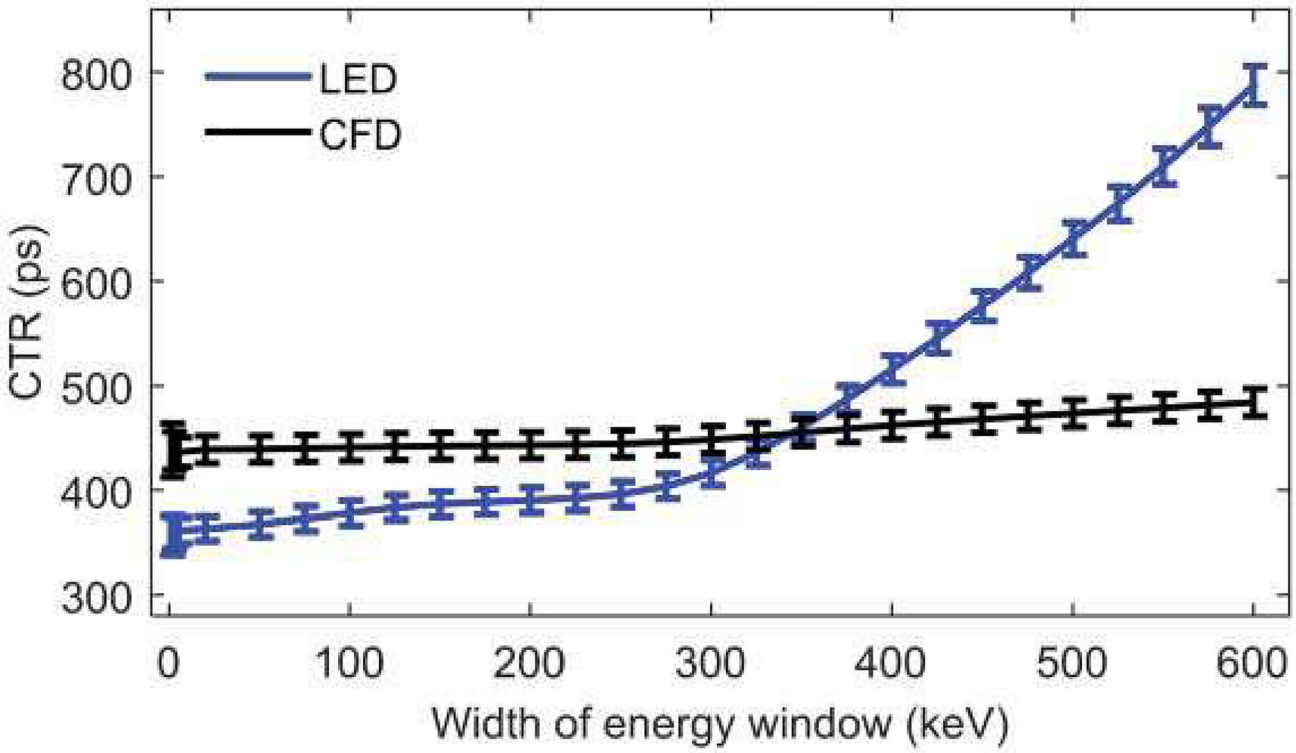

Fig. 4.

Timing resolution versus width of energy window. Timing resolution obtained using LED method is without time-walk correction. The error bars represent the uncertainty in the gaussian fit.

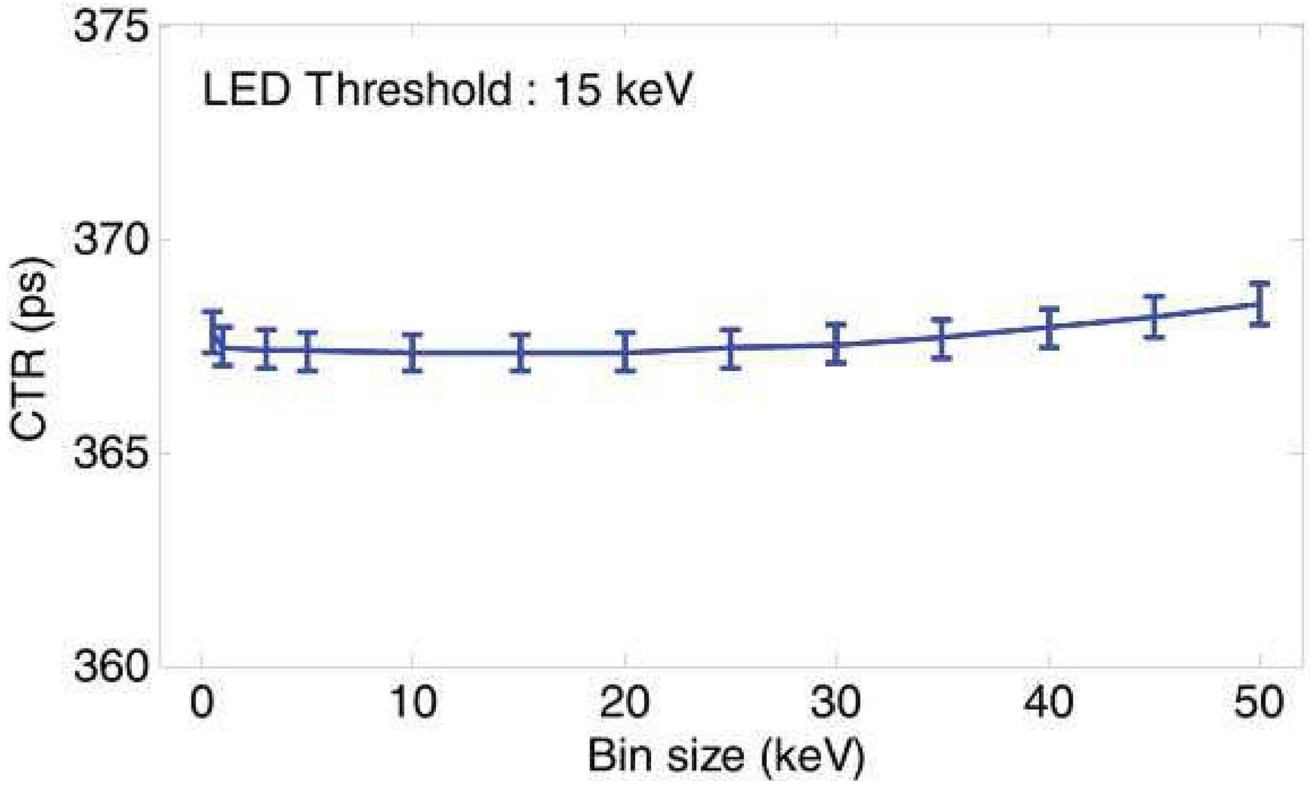

Fig. 5.

Energy bin size effect on timing resolution when threshold was 15 keV. A 425 keV – 650 keV energy window was applied to the data. The error bars represent the uncertainty in the gaussian fit.

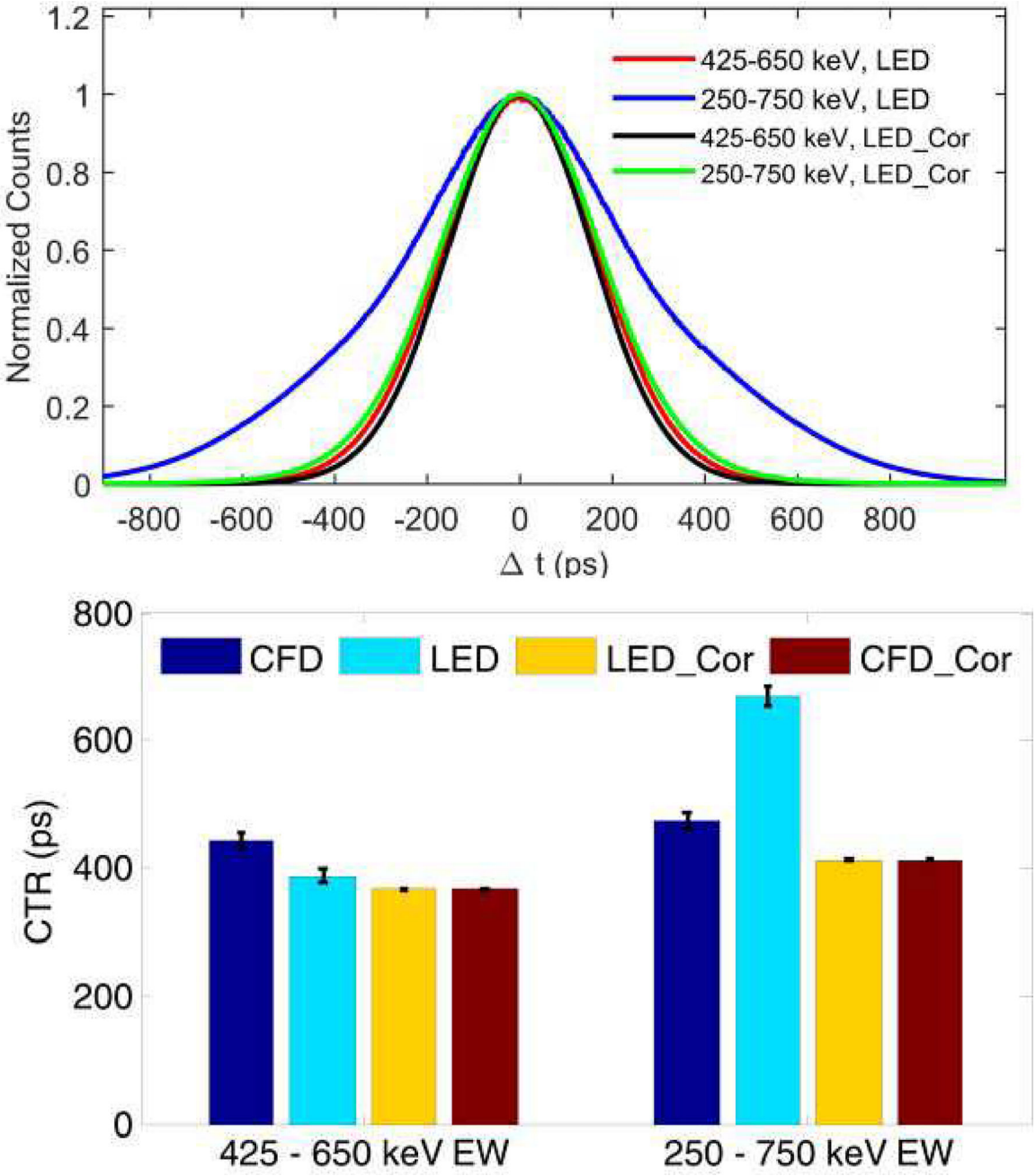

Fig. 6.

(top) Timing spectra obtained using LED technique, and (bottom) timing resolution obtained using different timing pick-off methods and different energy windows. The threshold of the LED is 15 keV.

TABLE I

Meaning of symbols in Fig.6, Fig. 7 and Table II

Symbol	Meaning
LED	LEDs were used for both detectors for time pick-off. Time-walk was not corrected.
CFD	CFDs were used for both detectors for time pick-off. A threshold was still applied before the CFD to reject low-energy events.
LED_Cor	LEDs were used for both detectors for time pick-off, but the time-walk was corrected using the proposed method for the target detector.
CFD_Cor	LED was used for target detector for time pick-off, whilst CFD was used for reference detector for time pick-off.

TABLE II

Timing Resolution Versus Threshold

Energy window (keV)	Method	Threshold[a] (keV)			
		15	100	200	300
425 – 625	CFD	442.8 ± 12.8 ps	442.8 ± 12.8 ps	442.8 ± 12.8 ps	441.5 ± 11.6 ps
	LED	389.0 ± 12.0 ps	847.3 ± 19.6	1739.9 ± 30.0 ps	3874.0 ± 41.5 ps
	LED_Cor	367.3 ± 0.5 ps	655.4 ± 0.7 ps	1238.2 ± 5.9 ps	2716.8 ± 4.7 ps
	CFD_Cor	367.3 ± 0.4 ps	656.5 ± 0.8 ps	1237.9 ± 6.0 ps	2716.7 ± 4.7 ps
250 – 750 [b]	CFD	476.0 ± 13.0 ps	476.0 ± 13.0 ps	476.0 ± 13.0 ps	472.8 ± 10.3 ps
	LED	670.2 ± 16.2 ps	1001.1 ± 27.9 ps	1821.2 ± 42.5ps	3933.4 ± 59.8 ps
	LED_Cor	413.7 ± 0.9 ps	781.4 ± 2.0 ps	1378.1 ± 6.0 ps	2834.7 ± 5.6 ps
	CFD_Cor	413.4 ± 0.9 ps	782.9 ± 2.1 ps	1383.0 ± 6.0 ps	2831.3 ± 5.3 ps

[a] Thresholds for CFD were the thresholds used to prevent the CFD triggering on low-energy events.

[b] 300 – 750 keV energy window was used to select the events when threshold is 300 keV.

IEEE Trans Radiat Plasma Med Sci. Author manuscript; available in PMC 2018 September 01.